

## Roles of silver oxide in the bipolar resistance switching devices with silver electrode

C. Y. Dong,<sup>1,2</sup> D. S. Shang,<sup>1,a)</sup> L. Shi,<sup>1</sup> J. R. Sun,<sup>1</sup> B. G. Shen,<sup>1</sup> F. Zhuge,<sup>3</sup> R. W. Li,<sup>3</sup> and W. Chen<sup>2</sup>

<sup>1</sup>Beijing National Laboratory for Condensed Matter Physics and Institute of Physics, Chinese Academy of Sciences, Beijing 100190, People's Republic of China

<sup>2</sup>Department of Physics, Hebei Normal University, Shijiazhuang 050016, People's Republic of China

<sup>3</sup>Ningbo Institute of Materials Technology and Engineering, Chinese Academy of Sciences, Ningbo 315201, People's Republic of China

(Received 22 November 2010; accepted 30 January 2011; published online 17 February 2011)

Three devices, Ag/WO<sub>3-x</sub>/Pt, Ag/AgO<sub>x</sub>/Pt, and Ag/AgO<sub>x</sub>/WO<sub>3-x</sub>/Pt, were investigated to elucidate the influence of the silver oxide on the bipolar resistive switching behavior. The silver oxide films were obtained by depositing silver at oxygen atmosphere. We find that the resistive switching behavior was determined by the silver oxide layer. Bulk and interface resistive switching were observed in the Ag/AgO<sub>x</sub>/Pt and Ag/AgO<sub>x</sub>/WO<sub>3-x</sub>/Pt devices, respectively. By the micro-x-ray photoemission spectroscopy analysis, it was demonstrated that the electrochemical redox reaction occurred in the AgO<sub>x</sub> layer is responsible for the resistive switching behavior at silver/oxide interface. © 2011 American Institute of Physics. [doi:10.1063/1.3556618]

Electric-pulse-induced resistive switching (RS) phenomena in metal/oxide/metal structure has recently attracted intensive attention due to its potential application in resistance random access memory (RRAM), a technique for the next generation nonvolatile memory.<sup>1,2</sup> Wide studies for the RS mechanism reveal that the RS occurs at the interface region between the electrode and oxide film.<sup>3-11</sup> The interface property is not only related with the selected electrode materials, but also with the electrode preparation techniques. Therefore, different researchers usually found different RS behaviors even for the same electrode and oxides. For instance, Shang *et al.*<sup>7,8</sup> and Fujimoto *et al.*<sup>9</sup> used silver paste as the top electrode and found that the Ag(paste)/La(or Pr)<sub>0.7</sub>Ca<sub>0.3</sub>MnO<sub>3</sub>/Pt devices exhibit *I-V* hysteresis and RS behavior. However, Sawa *et al.*<sup>10</sup> and Liao *et al.*<sup>11</sup> found no RS behavior in the Ag/Pr<sub>0.7</sub>Ca<sub>0.3</sub>MnO<sub>3</sub>/SrRuO<sub>3</sub> (or Pt) devices, in which the Ag top electrode was prepared by electron beam (or thermal evaporation) and magnetron sputtering. Recently, Yang *et al.* found hysteretic *I-V* curves and RS behavior in the Ag/La<sub>0.7</sub>Ca<sub>0.3</sub>MnO<sub>3</sub>/Pt devices, where Ag top electrode was deposited by electrobeam evaporation, and the RS endurance can be improved by alloying Al into the electrode.<sup>12</sup> These contradictions might be originated from the different chemical states of silver at the silver/oxide interface prepared by different techniques or technological conditions.

Silver is commonly used as an inert electrode material due to its antioxidation property. O<sub>2</sub> will be adsorbed dissociatively to form surface chemisorbed atomic oxygen, which is slowly incorporated into the silver bulk.<sup>13</sup> However, silver can be easily oxidized during the silver film deposition by thermal or electrobeam evaporation, sputtering, and pulsed laser deposition (PLD) of pure silver, if there is availability of oxygen in the growth chamber.<sup>14-19</sup> Moreover, much oxygen can be detected in the silver paste due to the existence of

epoxy. These remind us that silver oxidation might occur in the devices with RS behavior. The reported forms of silver oxide include the Ag<sub>2</sub>O, AgO, Ag<sub>3</sub>O<sub>4</sub>, Ag<sub>4</sub>O<sub>3</sub>, and Ag<sub>2</sub>O<sub>3</sub> phases. Among these oxides, the most thermodynamically stable oxide is Ag<sub>2</sub>O, which has a cubic structure and a *p*-type semiconducting character.<sup>18</sup> To clarify the effect of silver oxide on the RS behavior, in this letter, we prepared Ag electrode on Pt and WO<sub>3-x</sub>/Pt substrates by two steps: deposited first at oxygen atmosphere and second at vacuum condition. The RS behavior of the prepared devices was investigated, and the RS mechanism was discussed based on the redox of silver oxide.

A 250 nm WO<sub>3-x</sub> film was deposited on a Pt/Ti/SiO<sub>2</sub>/Si substrate at 400 °C under an oxygen partial pressure of 10 Pa by PLD. X-ray diffraction spectrum shows that the as-prepared WO<sub>3-x</sub> film is polycrystalline. A disklike AgO<sub>x</sub> film with a diameter of 100 μm defined by a metal mask was deposited by PLD from a pure silver target with an oxygen pressure of 10 Pa at room temperature on the as-prepared WO<sub>3</sub> film and Pt/Ti/SiO<sub>2</sub>/Si substrates. Subsequently, Ag top electrodes were *in situ* deposited on the AgO<sub>x</sub> film by PLD at room temperature under vacuum condition of 5 × 10<sup>-4</sup> Pa to form Ag/AgO<sub>x</sub>/WO<sub>3-x</sub>/Pt (AOWP) and Ag/AgO<sub>x</sub>/Pt (AOP) devices. The typical cross-sectional scanning electron microscopy (SEM) image of the prepared AOWP structure and the corresponding element mapping by an energy dispersive spectrometer (EDS) are shown in Fig. 1. Much oxygen element was detected in the Ag top layer near the WO<sub>3-x</sub> layer, where it should be corresponding to the AgO<sub>x</sub> layer, although the Ag and AgO<sub>x</sub> layers cannot be distinguished clearly from the SEM image. The whole thickness of the Ag/AgO<sub>x</sub> layer is ~180 nm. For comparison, we also prepared silver top electrodes directly on the WO<sub>3-x</sub> surface under the vacuum condition to form the Ag/WO<sub>3-x</sub>/Pt (AWP) devices. The chemical compositions of the Ag and AgO<sub>x</sub> surfaces were examined by x-ray photoemission spectroscopy (XPS) analysis (AXIS Ultra DLD, Shimadzu Corporation) with a monochromatic Al Kα line

<sup>a)</sup>Author to whom correspondence should be addressed. Electronic mail: shang\_da\_shan@163.com.

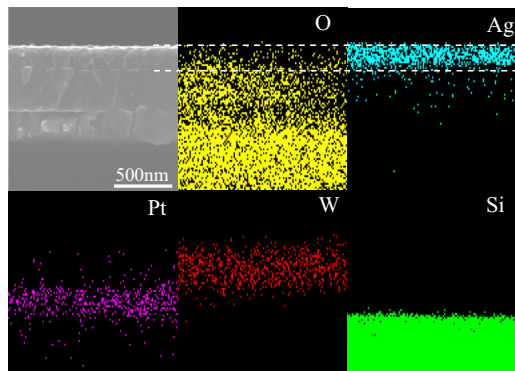


FIG. 1. (Color online) A typical cross-sectional SEM image of the prepared AOWP device and corresponding element mapping by EDS.

(beam-spot diameter of 110  $\mu\text{m}$ ).  $I$ - $V$  characteristics were measured by Keithley SourceMeter 2611 at the room temperature, using a standard two-probe technique. The electric bias directing from the Ag top electrode to the  $\text{WO}_{3-x}$  film is defined to be positive.

Figure 2 shows the XPS results of the deposited Ag and  $\text{AgO}_x$  films without covering the Ag top electrode layer. For the Ag film deposited at the vacuum condition, Ag  $3d$  peaks of the Ag film have the binding energy of 368.2 eV, which is the same value with that of pure Ag.<sup>20</sup> However, two weak O  $1s$  peaks also appeared at 530.4 and 532.1 eV. The O  $1s$  peaks in the pure Ag film should be due to an overlayer of the chemisorbed oxygen and coadsorbed  $\text{CO}_2$  covered under ambient conditions.<sup>21</sup> Comparing with the Ag film, Ag  $3d$  peaks of the  $\text{AgO}_x$  films have a shift of about 0.3 eV to the lower binding energy, which is opposite to that expected according to simple electronegativity arguments; however, it is consistent with previous reports about the transition of  $\text{Ag} \rightarrow \text{AgO}_x$ .<sup>20,21</sup> The anomalous chemical shift for silver oxide is determined by factors other than electronegativity differences such as lattice potential, work function changes, and extra-atomic relaxation energy and has been discussed by Gaarenstroom and Winograd.<sup>22</sup> Moreover, Ag  $3d$  peaks become broader with a full width at half-maximum (FWHM) from 0.6 eV (Ag) to 1.0 eV ( $\text{AgO}_x$ ). The broad Ag  $3d$  peak shape may be due to the presence of a mixture of  $\text{Ag}_2\text{O}$  and AgO or an intermediate oxide. However, the exact composition of the  $\text{AgO}_x$  film is difficult to be determined. The O/Ag atomic ratio calculated from the integrated intensity of Ag  $3d$  and O  $1s$  of the  $\text{AgO}_x$  film is about 1.5, which exceeds the theoretical stoichiometry expected for these compounds. That may be due to the presence of surface carbonate and other oxygen-containing species. The above transition was further confirmed by measuring the corresponding Ag  $MNN$  Auger spectra. As shown in Fig. 2(c), the maximum

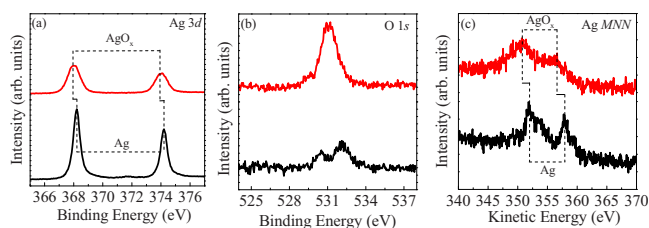


FIG. 2. (Color online) Respective XPS spectra of the (a) Ag  $3d$ , (b) O  $1s$ , and (c) Ag  $MNN$  Auger spectra obtained from the Ag and  $\text{AgO}_x$  film surfaces.

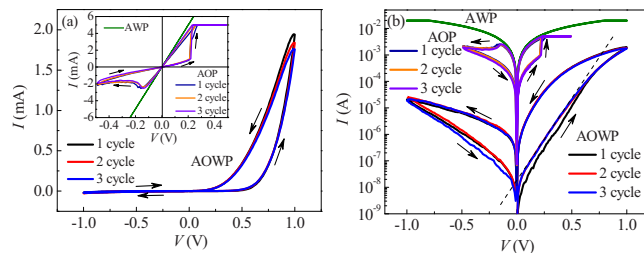


FIG. 3. (Color online)  $I$ - $V$  characteristics of the devices in (a) decimal and (b) semilogarithmic patterns.

Ag  $MNN$  peaks of the Ag film appears at a kinetic energy of 351.8 eV. Comparing the Ag  $MNN$  peaks of the  $\text{AgO}_x$  film with the Ag film peaks, a more obvious shift of 1.5 eV toward the lower kinetic energy can be observed, which is consistent with the  $\text{Ag} \rightarrow \text{Ag}_2\text{O}$  transition.<sup>20,21</sup> Therefore, we speculate that  $\text{Ag}_2\text{O}$  should be the main phase of the  $\text{AgO}_x$  layer.

$I$ - $V$  characteristics of the AWP, AOP, and AOWP devices are shown in Fig. 3. The AWP device exhibits a good linear Ohmic behavior with a resistance of  $\sim 40 \Omega$  [inset in Fig. 3(a)]. That is caused by the nonstoichiometry of the as-deposited  $\text{WO}_{3-x}$  film, where much oxygen vacancies exist resulting in a metalliclike transport property of the film.<sup>23</sup> In contrast, the  $I$ - $V$  curves of the AOP exhibit a pronounced  $I$ - $V$  hysteresis. An electroforming process by 0.5 V with current compliance of 5 mA is needed for the RS (not shown). From the hysteresis direction, it can be seen that the AOP device shows a bipolar RS behavior. The threshold voltage for RS is much lower than that reported in other transition metal oxides.<sup>3-11</sup> Both the high resistance state (HRS) and low resistance state (LRS) show Ohmic behavior. We define this type of RS without rectification feature in the HRS and LRS as the bulk RS relative to the interface RS with rectification. The  $I$ - $V$  curves of the AOWP device exhibit not only a pronounced  $I$ - $V$  hysteresis but also an obvious rectifying behavior. Comparing the  $I$ - $V$  curves with the AWP and AOP devices, the rectifying property of the AOWP should be originated from the barrier at the  $\text{AgO}_x/\text{WO}_{3-x}$  interface. As the most thermodynamically stable phases of the silver oxides,  $\text{Ag}_2\text{O}$  is a  $p$ -type semiconducting oxide,<sup>18</sup> while  $\text{WO}_{3-x}$  can be seen as a heavily doped  $n$ -type semiconducting oxide.<sup>22</sup> Therefore, it is possible for the  $\text{Ag}_2\text{O}/\text{WO}_{3-x}$  interface to form a  $p$ - $n$ -like heterojunction. This assumption was further confirmed by the linear semilogarithmic current at the positive bias, which can be fitted based on the thermionic emission theory:  $I \propto \exp(qV/nk_B T)$ , where  $q$  is the electron charge,  $n$  is the ideality factor, and  $k_B$  is the Boltzmann constant. According to the slope of the linear log  $I$ - $V$  curve [guided by a dashed line in Fig. 3(b)],  $n$  is calculated to be  $\sim 2.8$ , deviating significantly from the theoretical value of 1. Considering that the  $\text{AgO}_x$  layer should be composed of mixed phases and some uncertain reaction might occur at the  $\text{AgO}_x/\text{WO}_{3-x}$  interface, the deviation of  $n$  could be a consequence of spatial barrier inhomogeneities.<sup>24</sup> Therefore, the AOWP device resistance is dominated by the junction property, and the  $I$ - $V$  hysteresis should correspond to an interface RS behavior. Comparing the first cycle with subsequent cycles, only a slight shift was observed, suggesting that a weak electroforming process is required for the interface RS.

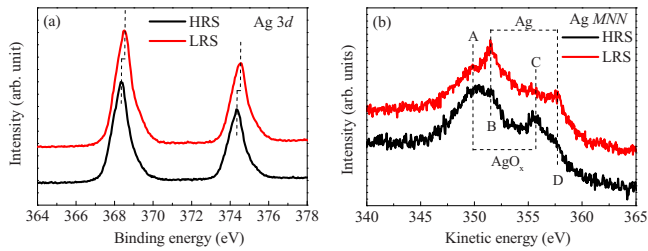


FIG. 4. (Color online) (a) Ag 3d XPS spectra and (b) Ag MNN Auger spectra obtained from the HRS and LRS of the AOWP device.

To clarify the role of silver oxide layer in the RS process, we investigated the chemical state of  $\text{AgO}_x$  at the HRS and LRS by micro-XPS analysis (beam-spot diameter of  $110 \mu\text{m}$ ). The Ag top electrode of the AOWP device was replaced with an Ag probe with a diameter of  $\sim 20 \mu\text{m}$ , which was contacted directly with the  $\text{AgO}_x$  surface and was removed after each electric field trigger. Then, the HRS and LRS were separately obtained on each disklike  $\text{AgO}_x$  layer. Tens of RS triggers were performed at different positions around the  $\text{AgO}_x$  disk center to ensure the reliability of the XPS measurement. As shown in Fig. 4(a), a little change of intensity and FWHM of Ag 3d core level peaks can be observed, although a negligible shift ( $\sim 0.15 \text{ eV}$ ) of Ag 3d peaks toward higher binding energy appeared in the LRS. In view of the resolution ( $0.1 \text{ eV}$ ) of the micro-XPS we used, these results mean that either the chemical state of  $\text{AgO}_x$  did not change during the RS or the change amount of  $\text{AgO}_x$  was too slight to be detected. The chemical state of  $\text{AgO}_x$  was further confirmed by measuring the change of Ag MNN Auger spectra, which would exhibit larger energy shifts and shape changes than the XPS Ag 3d peaks with varying chemical state because a single Auger transition involves three electrons and many-body effects.<sup>20,21</sup> From Fig. 4(b), we can see that four main peaks, denoted by A, B, C, and D, appeared at both the HRS and LRS. Peaks A and C correspond to  $\text{AgO}_x$  and peaks B and D correspond to Ag. Intensities of peaks A and C decreased, while intensities of peaks B and D increased, indicating that the content of  $\text{AgO}_x$  (Ag) in the  $\text{AgO}_x$  layer decreased (increased) with the RS from HRS to LRS. The same results were also obtained in measurement of the AOP devices. These changes of Ag MNN Auger peaks further confirm the electrochemical redox reaction of  $\text{AgO}_x$  during the RS.

Based on the above results, we assume that silver and oxygen ions were driven to the two opposite sides of the  $\text{AgO}_x$  film by the electric field and then decomposed into metallic silver and O atoms. Under the positive bias, the former was left in the film, while the latter dissolved in the Ag top electrode or was released into atmosphere in the form of  $\text{O}_2$ . For the AOWP device, the metallic silver would damage the  $\text{AgO}_x/\text{WO}_{3-x}$  interface barrier, resulting in the decrease of device resistance. For the AOP device, since no interface barrier existed, the metallic silver would form conductive channels, resulting in the LRS with Ohmic transport behavior. Under the negative bias, the metallic silver was reoxidized and the devices restored to the HRS again. Moreover, the current-induced Joule heating effect should play an assistant role to the redox of the  $\text{AgO}_x$  layer. As we know,

the thermal stability of silver oxides is weak since they will be decomposed into metallic silver and  $\text{O}_2$  at around 573–763 K in air.<sup>21</sup> This thermodynamic property of silver oxides might be propitious to fabricate RRAM devices with lower power consumption.

In conclusion, our investigation of the  $I$ - $V$  characteristics and silver chemical states of three devices, AWP ( $\text{Ag}/\text{WO}_{3-x}/\text{Pt}$ ), AOP ( $\text{Ag}/\text{AgO}_x/\text{Pt}$ ), and AOWP ( $\text{Ag}/\text{AgO}_x/\text{WO}_{3-x}/\text{Pt}$ ), showed that the RS behavior was driven by the electrochemical redox reaction of the silver oxide layer. Bulk and interface RS were observed in the AOP and AOWP devices, respectively. The present results suggest that the redox reaction of metal electrode plays an important role in the RS behavior and should draw more attention for investigating the electrical properties of metal/oxide interfaces.

This work was supported by the National Basic Research of China, the National Natural Science Foundation of China, the Knowledge Innovation Project of the Chinese Academy of Sciences, and the Beijing Municipal Nature Science Foundation.

- <sup>1</sup>R. Waser, R. Dittmann, G. Staikov, and K. Szot, *Adv. Mater.* **21**, 2632 (2009).
- <sup>2</sup>A. Sawa, *Mater. Today* **11**, 28 (2008).
- <sup>3</sup>A. Baikalov, Y. Q. Wang, B. Shen, B. Lorenz, S. Tsui, Y. Y. Sun, Y. Y. Xue, and C. W. Chu, *Appl. Phys. Lett.* **83**, 957 (2003).
- <sup>4</sup>Y. B. Nian, J. Strozier, N. J. Wu, X. Chen, and A. Ignatiev, *Phys. Rev. Lett.* **98**, 146403 (2007).
- <sup>5</sup>J. J. Yang, M. D. Pickett, X. M. Li, D. A. A. Ohlberg, D. R. Steward, and R. S. Williams, *Nat. Nanotechnol.* **3**, 429 (2008).
- <sup>6</sup>R. Yasuhara, T. Yamamoto, I. Ohkubo, H. Kumigashira, and M. Oshima, *Appl. Phys. Lett.* **97**, 132111 (2010).
- <sup>7</sup>D. S. Shang, Q. Wang, L. D. Chen, R. Dong, X. M. Li, and W. Q. Zhang, *Phys. Rev. B* **73**, 245427 (2006).
- <sup>8</sup>D. S. Shang, L. D. Chen, Q. Wang, Z. H. Wu, W. Q. Zhang, and X. M. Li, *J. Mater. Res.* **23**, 302 (2008).
- <sup>9</sup>M. Fujimoto, H. Koyama, Y. Nishi, and T. Suzuki, *Appl. Phys. Lett.* **91**, 223504 (2007).
- <sup>10</sup>A. Sawa, T. Fujii, M. Kawasaki, and Y. Tokura, *Appl. Phys. Lett.* **88**, 232112 (2006).
- <sup>11</sup>Z. L. Liao, Z. Z. Wang, Y. Meng, Z. Y. Liu, P. Gao, J. L. Gang, H. W. Zhao, X. J. Liang, X. D. Bai, and D. M. Chen, *Appl. Phys. Lett.* **94**, 253503 (2009).
- <sup>12</sup>R. Yang, X. M. Li, W. D. Yu, X. D. Gao, D. S. Shang, and L. D. Chen, *J. Appl. Phys.* **107**, 063703 (2010).
- <sup>13</sup>C. I. Carlisle, T. Fujimoto, W. S. Sim, and D. A. King, *Surf. Sci.* **470**, 15 (2000).
- <sup>14</sup>L. A. A. Pettersson and P. G. Snyder, *Thin Solid Films* **270**, 69 (1995).
- <sup>15</sup>F. X. Bock, T. M. Christensen, S. B. Rivers, L. D. Doucette, and R. J. Lad, *Thin Solid Films* **468**, 57 (2004).
- <sup>16</sup>D. Büchel, C. Mihalcea, T. Fukaya, N. Atoda, J. Tominaga, T. Kikuwa, and H. Fuji, *Appl. Phys. Lett.* **79**, 620 (2001).
- <sup>17</sup>N. R. C. Raju, K. J. Kumar, and A. Subrahmanyam, *J. Phys. D: Appl. Phys.* **42**, 135411 (2009).
- <sup>18</sup>U. K. Barika, S. Srinivasan, C. L. Nagendra, and A. Subrahmanyam, *Thin Solid Films* **429**, 129 (2003).
- <sup>19</sup>J. F. Pierson and C. Rousselot, *Surf. Coat. Technol.* **200**, 276 (2005).
- <sup>20</sup>L. H. Tjeng, M. B. J. Meinders, J. van Elp, J. Ghijsen, G. A. Sawatzky, and R. L. Johnson, *Phys. Rev. B* **41**, 3190 (1990).
- <sup>21</sup>J. F. Weaver and G. B. Hoflund, *Chem. Mater.* **6**, 1693 (1994); *J. Phys. Chem.* **98**, 8519 (1994).
- <sup>22</sup>S. W. Gaarenstroom and N. Winograd, *J. Chem. Phys.* **67**, 3500 (1977).
- <sup>23</sup>M. Gillet, C. Lemire, E. Gillet, and K. Aguir, *Surf. Sci.* **532–535**, 519 (2003).
- <sup>24</sup>J. H. Werner and H. H. Güttler, *J. Appl. Phys.* **69**, 1522 (1991).